# Multiphysics Based Thermal Modeling of a Pouch Lithium-Ion Battery Cell for the Development of Pack Level Thermal Management System

Khan, Mohammad Rezwan; Kær, Søren Knudsen

*Published in:*
Proceedings of 2016 Eleventh International Conference on Ecological Vehicles and Renewable Energies (EVER)

*DOI (link to publication from Publisher):*
10.1109/EVER.2016.7476442

*Publication date:*
2016

*Document Version*
Early version, also known as pre-print

2016 Eleventh International Conference on Ecological Vehicles and Renewable Energies (EVER)

# Multiphysics Based Thermal Modeling of a Pouch Lithium-Ion Battery Cell for the Development of Pack Level Thermal Management System

Mohammad Rezwan Khan, Søren Knudsen Kær
Department of Energy Technology, Pontoppidanstræde 101, Aalborg University, DK-9220, Aalborg,Denmark.
Email: rezwankhn@gmail.com;mrk@et.aau.dk

*Abstract*— **The research is focused on the development of a three-dimensional cell level multiphysics battery thermal model. The primary aim is to represent the cooling mechanism inside the unit cell battery pack. It is accomplished through the coupling of heat transfer and computational fluid dynamics (CFD) physics. A lumped value of heat generation (HG) inside the battery cell is used. It stems from isothermal calorimeter experiment. HG depends on current rate and the corresponding operating temperature. It is demonstrated that the developed model provides a deeper understanding of the thermal spatio-temporal behavior of Li-ion battery in different operating conditions.**

***Keywords— Surface temperature; spatial and temporal temperature distribution: Isothermal Calorimeter; Lithium Titanate Oxide; Battery thermal management; heat generation; Battery performance; three dimesional multiphysics model;CFD.***

## I. INTRODUCTION

Electric vehicles (EV) and stationary batteries are associated with high continuous loads. It leads to higher temperature rise inside the battery pack. These phenomena are well known from the tests and empirical field data that the reliability and lifetime performance of battery packs are mainly temperature related [1, 2]. Moreover, the current trend is now towards the use of the increasingly high performance, and high power batteries inside the pack with dense packaging. Additionally, different peripherals are placed in a tight manner due to space constraints, so there is not enough space for natural circulation of air and the associated heat removal. These thermal related challenges are the limiting factor for the application performance.

The effect of temperature change on the different conditions of a set of battery cells in a pack setting is reflected in the previous instances of different model related literature [3-5]. It is shown how different operating conditions (e.g., unbalanced state of charge (SoC) [6, 7], various ageing conditions [8, 9], flow rates [10, 11], etc.) may affect battery cells' performance and may cause thermal gradients [12-16]. Besides, it should be noted that every sub-class of lithium ion cell chemistry shows both endothermic and exothermic components [3, 8, 17, 18]. For this reason, heat flux measurement using, for example, a calorimeter is crucial to determine the real heat generation inside the cell.

Additionally, the temperature dependence of HG causes the performance of the battery to be strongly dependent on thermal management [13, 15, 19-23].The failure to take necessary steps can promote failures at the battery package [24]. A prerequisite for an effective BTMS is an accurate thermal model. Even though the various aspects of performance required from a battery regarding power and energy can be assessed experimentally, battery modeling can be of valuable use to explore various thermal and cooling limitations [1-3]. In this way, it helps to find the required specifications and configurations of BTMS for the better battery system performance. To model the non-uniformity of the cell temperature, several modelling methods have been adopted [24-30]. Moreover, the effectiveness and limitations of these methods are concisely discussed from the thermal behavior of the investigated cells in different review literature [31, 32].

Modelling the thermal dynamics of the battery system is not trivial due to the multidisciplinary science and engineering requirements. There exists a countless amount of configuration of the underlying system and cooling process in both cell and pack setting. So, from a general

thermal research point of view, it is a necessity that the modelling method should be coherent and general enough to handle a wide variety of thermal problems inside the battery pack.

In this research, there is an attempt to trace the thermal gradients inside the unit battery cell pack using multi-physics analysis. Section II presents the methodology for this investigation. The electro-thermal modelling of the cell and underlying theoretical considerations, hypotheses, the mathematical structure, thermal modeling steps, used tools and meshing recommendation are elaborated in Section III. It consists of a 3D model that couples the heat transfer problem of the battery with the forced convection problem within the heat transfer fluid air, of the unit cell pack. The simulation result of the electro-thermal modelling of the surface temperature is presented in Section IV. It includes the experimental adjustment of the model. The simulation is performed with a focus on the HG and temperature distribution over the surface of the battery cell that has an exposure of cooling fluid. Then, thermal model predictions are presented and compared with various operating conditions. In the end, the conclusions of the research are presented in Section V.

## II. Methodology

The objective is to develop a simplified and computationally efficient multiphysics-based thermal model of unit cell Li-ion battery pack. It integrates the main design parameters of the battery cell (such as dimensions, materials, and corresponding physical parameters) and relevant physics (heat transfer and computational fluid dynamics (CFD)). The modelling procedure is composed of three stages. Those are pre-processing, solution of the model, and post-processing respectively.

At the pre-processing stage, the battery geometry is analyzed and generated in a suitable manner for further analysis. The relevant physics dependent parameter values and corresponding operational settings are inserted as input parameters. Then relevant physics are stipulated over the different material.

At solution of the model stage, the thermal time-dependent and steady state problem with cooling is solved numerically by considering the heat generation in the battery as a bulk heat source. The battery cell has direct exposure to a cooling medium air. The cell has anisotropic properties. So, a uniform defined initial temperature is imposed on the corresponding boundaries. Thereafter, other essential boundary conditions are introduced. The amount of heat source generation (inside LTO cell corresponding to the current rate) is measured by an isothermal calorimeter and used as an input to the thermal model. When the battery is operational, it suddenly releases a finite, uniform and constant quantity of heat energy in the surrounding air. There is an unobstructed propagation of the heat energy in the longitudinal (x), lateral (y) and normal (z) directions. Then, the whole domain is broken down into a suitable mesh for solving through finite element method (FEM) technique. The next step is to solve the model using commercial FEM software. The final result of the model is the determination of temperature spatio-temporal distribution and the amount of heat generation of the battery cell under cycling condition. In the post-processing stage, the results are compared with a series of associated outputs.

## III. Model

The presented model considers a unit cell based pack i.e. a standalone pack that contains only a single battery cell. It takes into account the heat transfer using fundamental thermodynamics and cooling mechanisms due to the surrounding flow that is considered laminar.

### *A. Geometry*

The studied unit battery cell is a large-size pouch lithium titanate (LTO) cell having 13Ah nominal capacity. The geometries are found from careful measurement of the battery in the laboratory. The corresponding cell geometry is represented in Fig. 1.

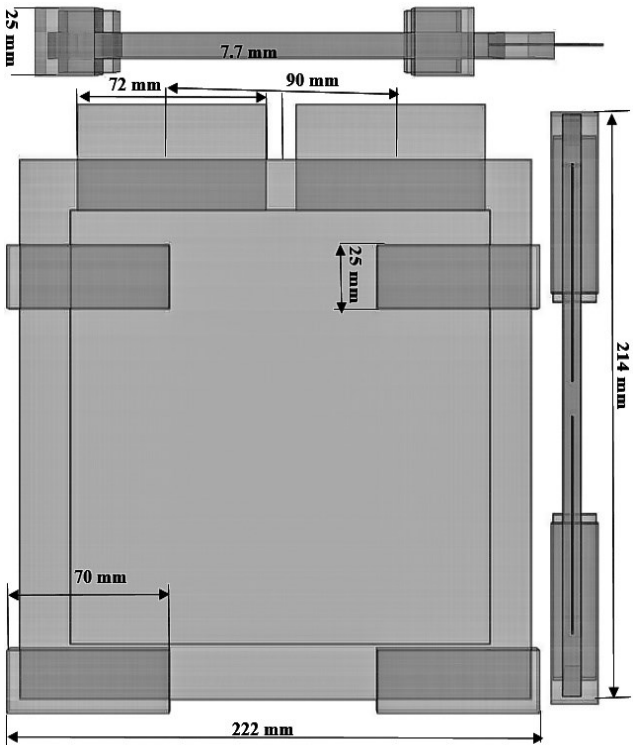


Fig. 1. Analysis of the LTO battery cell in a different orientation.

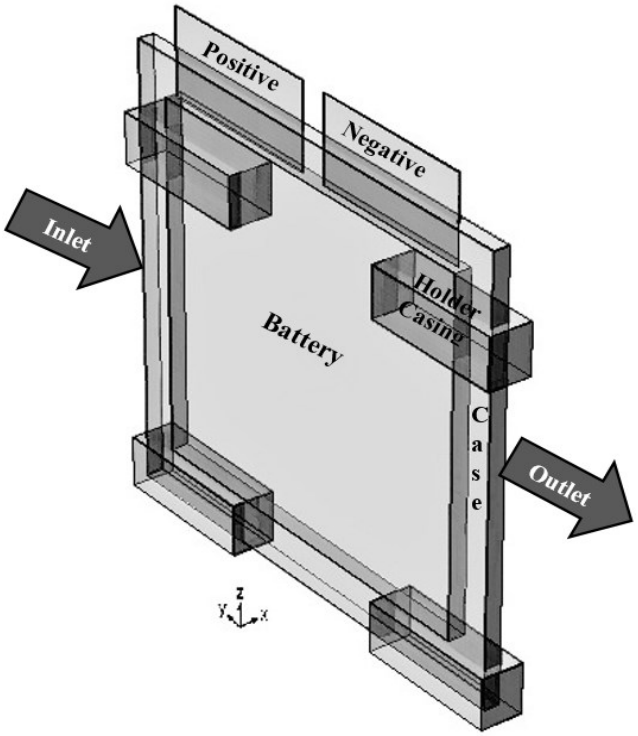


Fig. 2. Geometrical segmentation and experimental condition of the cell.

### B. Parameters and Physical Properties

The unit cell battery module is composed of a battery, case, positive and negative electrode as well as holder casing as shown in Fig. 2. Naturally in a 3D battery model, three modelling space is considered. The electrical and physical properties needed for the model are given in TABLE II.

The next step is to introduce and to define the suitable physical properties of the materials in the different domain of the model (associated with the corresponding geometry). The underlying physics of the 3D battery model is heat transfer and CFD. Moreover, there are a set of parameters that include the battery materials properties, the external environment, and other influencing conditions as shown in TABLE II. In a steady-state solution to a 3D model, parameters can vary only as a function of position in space ($x$), space ($y$), and space ($z$) coordinates, while in case of time dependent solution there is an addition of time dependence. There is an air flow from one side of the battery, and there is only one outlet available to pass through this air.

### C. Assumptions and Boundary conditions

For the interface between battery surface and air flow channel, coupled boundary conditions satisfy the continuity of temperature profiles at the boundary line. It means that it couples the conductive heat transport towards the cell surface with the corresponding heat transport by convection at the surface. The same coupling is defined for both terminals on the Li-ion cell. This model only considers transport of heat by conduction inside the battery and forced convection for the cooling medium air. This is a simplification of the thermal effects inside a pack setting, for instance, other heat sources can be present such as heat emitted from cabin heating system, heat generation from power electronics and peripherals, etc. [33, 34].

The following additional significant assumptions are used to reach a solution. Those are categorized according to physics:

#### 1) Heat Transfer Assumptions

The thermal properties of the fluid and battery are homogeneous. So those remain constant unless stated otherwise. There is negligible radiative energy transfer, and it is not accounted for. Forced convection is the dominant process for heat transfer from the terminal surfaces. An average specific heat for the cell is employed in the simulation in steady state and time dependent situation as the approximation of real life measurement. It is assumed that the battery is a non-uniform and anisotropic medium with different thermal conductivity in each coordinate direction ($k_{\mathrm{xx}}, k_{\mathrm{yy}}, k_{\mathrm{zz}}$) as shown in TABLE II. It also contains specific capacity of the battery and density that are taken from existing literature. The temperature at the inlet section of the battery pack remains constant.

In this study, different values for the volumetric heat generation are considered as measured by a calorimeter for the different load profiles. This is the only heat generation source that comes from the Li-ion cell. The generated heat is spatially uniform inside the battery domain. The calorimetric measurement obtains heat generation in the cell.

#### 2) CFD Assumptions

The flow of incompressible heat transfer fluid is assumed as laminar. The normal stress at the inlet of the system is determined from the flow conditions at the entrance to a fictitious channel of length one meter appended to the boundary.

### D. Mathematical description of the model

The thermal model is developed by setting up a generic energy balance equation that accounts for accumulated, conducted and generated local heats and the cooling process as described by [33-36].

Thermal models describe the thermal behavior regarding heating of the battery and are built on the energy conservation of the system as follows in Eqn. (1)

$$\rho C_p \frac{\partial T}{\partial t} = k\nabla^2 T + Q \quad (1)$$

where, $T$ —temperature of the system domain, ρ—density of the system component, $C_p$—specific heat capacity, $k$ —thermal conductivity and $Q$ — the local heat generation having a volumetric heat source.

In this modelling framework, for the macroscopic geometrical level of the battery cell is divided primarily into three domains: electrode, tab (positive and negative) and casing (Refer to Fig. 2). Different domains are given, and different material attributes are associated. Thus, Equations for the three respective domains are presented in Eqn.(2) and (4) respectively:

*a) Steady state and time dependent equations*

**For Casing:**

$$\rho C_p \frac{\partial T}{\partial t} + \rho C_p . \nabla T + \nabla . q = Q, \quad (2)$$

$$q = -k\nabla T \quad (3)$$

**Electrode and tab domain:**

$$\rho C_p \frac{\partial T}{\partial t} = k\nabla^2 T + Q, \quad (4)$$

**The CFD equations** are presented in Eqn.(5) and (6):

$$\frac{\partial u}{\partial t} + \rho(u.\nabla)u = \nabla.(-\mathrm{pI} + \mu(\nabla u + (\nabla u)^T)) \quad (5)$$

$$\rho\nabla.(u) = 0, \quad (6)$$

where

$\rho$ is the density.

$u$ is the velocity vector.

The finite element method (FEM) is employed in this study to discretize the governing equations. Depending on the level of the modelling, these modelling equations are applied to the separate domains of the battery.

### *E. Meshing, Discretization, and Solver selection*

To achieve the appropriate results from a simulation, it is required to accomplish the diverse type of procedures as required for FEM, for instance, mesh generation, discretization, and selection of proper solvers. To address these issues, Comsol® Multiphysics™ software environment is used.

The meshing of the geometry is illustrated in Fig. 3. Boundary layers are employed since there is a high-velocity gradient at the interface between the battery surface and the cooling medium and it is important for the heat transfer calculation. A swept mesh is employed. Mesh sweeping operates on the 3D domain by first meshing a source face of the battery. Then it sweeps the resulting face mesh through the domain to an opposite destination face. All the faces that encompass the planes of the battery are classified as either source faces or a destination face or linking faces. The linking faces of the battery are the faces that connect the source and destination faces. So, the sources for the swept mesh consist of several faces.

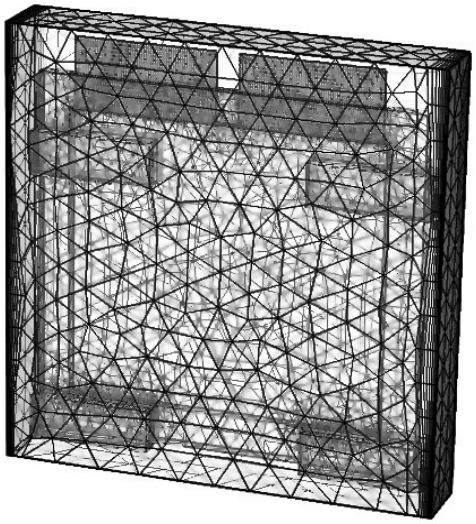

Fig. 3. Meshing of the geometry. Boundary layer meshes are on the boundary of the control volume. Free triangular and free tetrahedral are used on the battery surface.

Additionally, for solving the governing equations, the geometric multigrid solver is employed. It accelerates the convergence of the iterative solver by solving the FEM problem on a series of meshes rather than a single one. The multigrid algorithm starts with the initial physics controlled mesh and automatically builds a series of coarser meshes. The process is repeated until the coarsest mesh leads to a low enough number of degrees of freedom.

## IV. Result and Discussion

To assist the proposed modelling approach, calorimetric experiments are performed. Using the amount of heat generation measured by the calorimeter, the model is simulated to exhibit the temperature distribution (to trace the temperature gradient) in the cooling condition.

### *A. Experimental*

A battery cycler has been used to charge the battery until the maximum voltage (Vmax= 2.80 V corresponding to 100% SoC) and to discharge it until the cut-off voltage (Vmin=1.50V corresponding to 0% SoC). This is accomplished at both 1C and 2C current rate. To analyze the temperature distribution over the surface of the battery, four thermocouples (K-type) have been placed as shown in Fig. 4. The unit cell module is placed in a hermetically closed environment initially at 27°C. A large commercial isothermal calorimeter IBC 284 manufactured by

Netzsch™ is employed for heat flux measurement. The detailed experimental setup, as well as corresponding materials and equipment, can be found in [37].

### *B. Temperature Spatial Distribution and Influence of the Cooling*

The model can predict the surface temperature distribution of the battery at different operating conditions. The model is simulated in both steady state and time dependent environment to find the temperature spatial distribution over the surface. The modelling scheme is also used to demonstrate the influence of cooling.

### *C. Steady State result*

The simulation is carried out at 2C current rate equivalent to 5137mW heat generation from the battery. The steady-state simulation is pursued. Fig. 5 illustrates the distributions of the temperature over the surface of the cell. ). For cooling purposes, a 1m/s air flux is entering at 27°C on the inlet side of the module. According to the observation, the temperature rose sharply to a common point. As expected, the location of the hottest region is observed near the outlet position of the unit cell module throughout the discharge process (far end of the cooling liquid air). The non-uniform heat propagation is also observed. At the end of the cycling, it indicates lower temperatures (around 28°C) at the front near the inlet and higher temperatures (around 34°C) at the rear of the unit cell module. The stationary thermal model is associated with constant heat generation. The unit cell module with the cooling system reaches to an equilibrium between the total temperature difference depending on the amount of heat generation and the cooling flow velocity. The cooling allows a limited temperature increase so that additional exothermic reactions cannot be initiated. Thus, the heat production cannot go out of control. By this way thermal runaway is avoided.

At low current rates, the evolutions of the maximum temperature of the cell is restricted. The phenomenon reflects the small increases in the surface temperature. Fast equilibrium is reached during low current rates. By this way, there is a parity between the heat generated inside the cells and the heat removed out of the cells. On the other hand, with the increase in the current rate, the temperature contours show steeper slopes. It indicates faster temperature rise during the discharge of the cells. This is because of the greater amount of heat generated inside the cells at high current rates. It prevents the cells from achieving equilibrium in a shorter time. As shown in TABLE I. , the temperature at each surface has different value implying temperature gradient. From the modelling analysis in different current rates, the variation of heat generation and temperature gradients in four specific points are found. The analysis shows, there is a significant (217%) rise in heat generation in 1C cycling to 2C cycling.

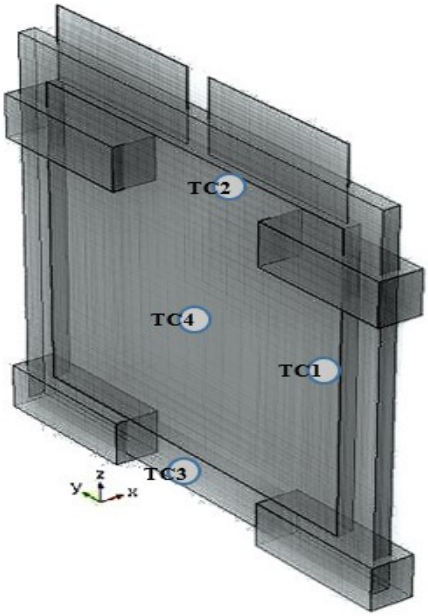


Fig. 4. Thermocouple placement over the surface of the battery.

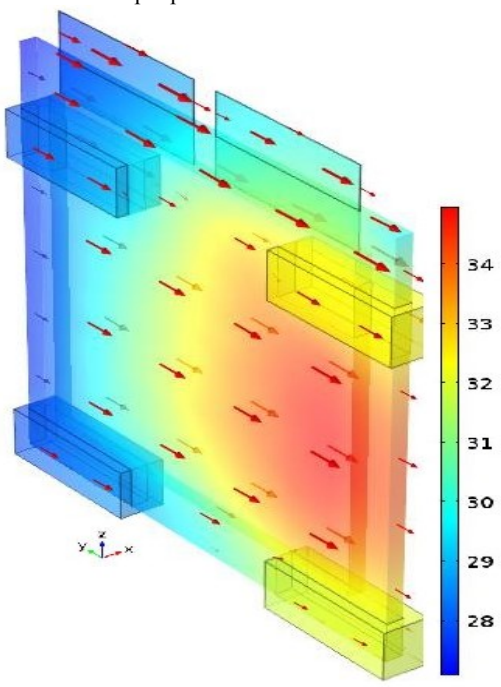


Fig. 5. Temperature distribution is shown within a unit single cell pack with the cooling system. The impact of 2C charge and discharge is shown. Additionally, there is an airflow from left directions to right (in arrow plot). The temperature of the ambience around the cells has increased significantly due to increase in heat generation. There is a visible cooling effect near inlet due to the carrier flow (showing less temperature) and the opposite is true near the outlet.

TABLE I. SIMULATION RESULT OF THE MODEL AT THE DIFFERENT CURRENT RATE.

| Attribute | 1C Model result | 2C Model result | % change from 1C to 2C cycling |
|---|---|---|---|
| Thermocouple 1 (°C) | 31.5 | 33.5 | 6.35 |
| Thermocouple 2 (°C) | 30.1 | 30.5 | 1.33 |
| Thermocouple 3 (°C) | 28.5 | 29.9 | 4.91 |
| Thermocouple 4 (°C) | 31.6 | 32.5 | 2.85 |
| Heat Generation (mW) | 1621 | 5137 | 217 |

As the current rate increases (1C to 2C), higher temperature gradients at the cell surfaces are observed (Refer to TABLE I. ). Consequently, thermal management can play an important role to avoid too large temperature increase of the surrounding of the cell, especially during the charge and discharge of a module at high current rates. Since those certainly exhibit higher gradient due to high amount of heat generation. The rationale of the phenomena is that the temperature gradient causes portions of the cell to generate more current (electrochemically reaction rate is increased). This causes these hotter sections to increase further in temperature. So this positive current temperature feedback can be countered by airflow that flows from the inlet. Even if the high rate charging takes place only for a short part of the lifetime of a battery, the developed thermal gradients imposed can be lowered with the right selection of carrier fluid velocity to keep the thermal states constant. Higher gradient scenarios can be avoided by taking preventive action by cooling.

*1) Influence of the Air velocity*

Fig. 6 illustrates the surface temperature distribution in a unit cell battery module at the end of 1C discharge with a low (left) and a high (right) velocity. The module is kept initially at 27°C and is closed in hermetic enclosure.It demonstrates the cooling of a battery module discharged with 1C current rate. For cooling purposes, a 1m/s air flux is entering at 27°C on the inlet side of the module. At the end of the discharge, Figure indicates lower temperatures (around 27°C) at the front and higher temperatures (around 30-31°C) at the rear of the unit cell module. With an increased air flux equal to 2 m/s, as compared to low velocity figure, a better cooling of the cells is achieved. The simulation case considers the same initial thermal conditions. Therefore, the figure emphasizes the need for a sufficient cooling for a proper thermal management of the pack. Hence, thermal management is important to avoid too large of an increase in the temperature of the air surrounding the cells, especially during the discharge of a module at high current rates.

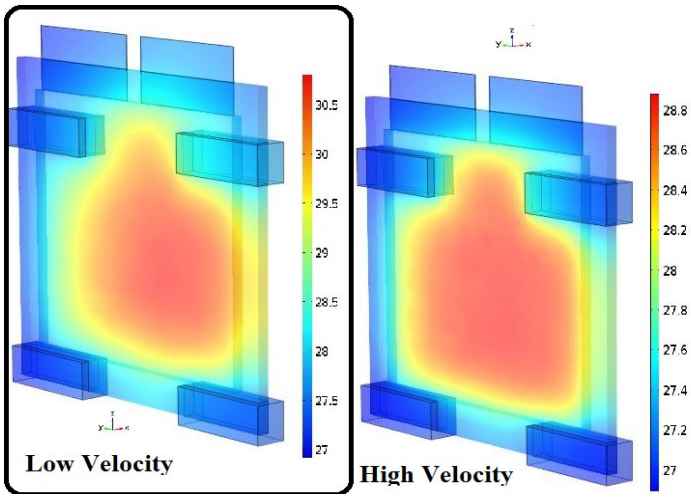


Fig. 6. Effect of velocity on temperature diustribution of the battery cell surface. [Left]Low velocity 1m/s air flux is entering at 27°C on the inlet side of the module; . [Right] High velocity 2m/s air flux is entering at 27°C on the inlet side of the module.

*D. Time dependent result*

A time-dependent model is built using the methodology as steady state case to investigate transient behavior. The temporal battery temperature distribution of the battery pack is revealed in Fig. 7. Variations in temperature profiles between the different types are observed during continuous discharge at 1C current rate. When heat is generated inside the unit battery cell pack, internal temperature gradients will necessarily emerge with time.

Considering cooling the battery with air, an ambient temperature difference in the air of around 30-31°C is likely in this current rate with the cooling rate. Hence, the battery temperature is manageable with higher velocity.The figure shows modelled spatio-temporal temperature profiles. Deploying the given model along with the associated parameters coupled with the relevant physics some insight of the thermal gradient evolution can be found. Subsequently, it helps to prevent these temperature gradients with a proper cooling mechanism.

The proposed model is built on numerical methods that that are extremely useful to understand the thermal and cooling phenomena of a unit cell battery. Moreover, by taking the 3D modelling trajectory, it is ensured the solution is more future-proof than other reduced dimensional (lumped or 0D, 1D,2D) counterparts. On the contrary to the empirical modeling approaches, the presented physics-based model can provide detailed information of spatio-temporal temperature distribution. Moreover, it can be used more promisingly to compare candidate solutions for cooling model simulation. Likewise, because of FEM related models are used in the

research, it can be used readily for the coupling with other physics, for instance, electrochemical modelling.

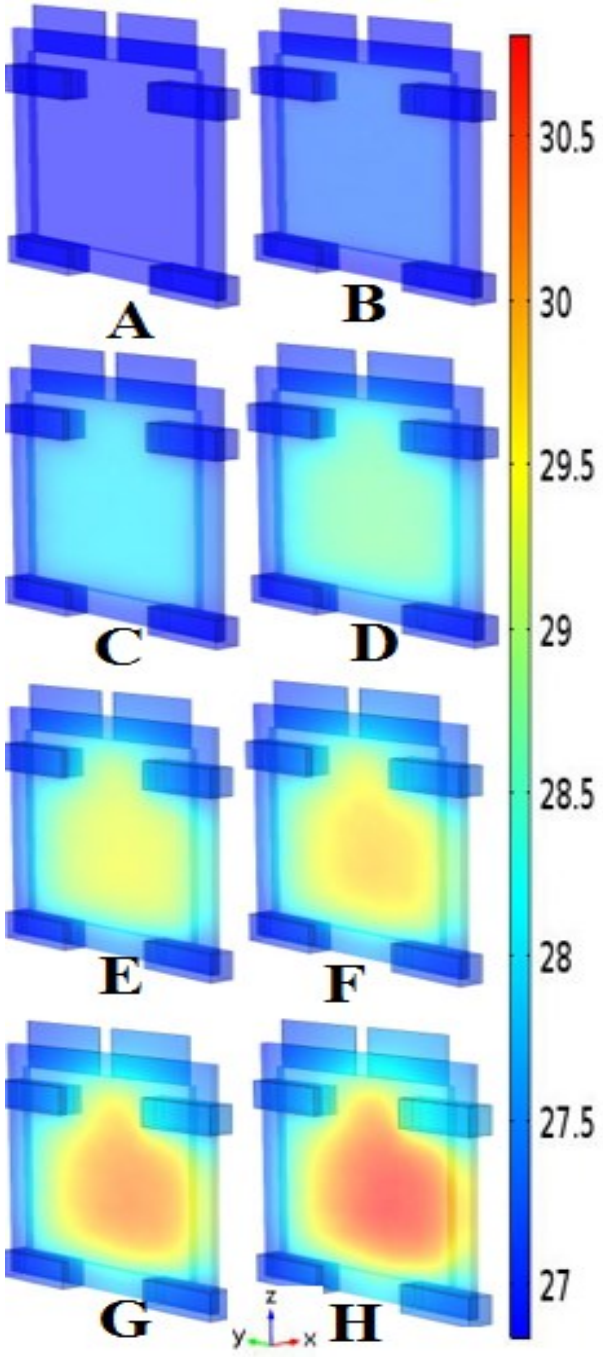


Fig. 7. Transient simulation results of the battery pack with a cell with 1C discharge with 1m/s air flux and 27°C initial temperature in alphabetic caption order.There is significant temeperature gradient with the time evolution.[A]0 sec [B]7 min 30 Sec [C] 15 min [D] 22 min 30 Sec [E] 30 min [F] 37 min 30 Sec [G] 45 min 30 Sec [H] 60 min .

The used approach does not require detail knowledge of the component materials of the particular cell as a bulk approximation is used. So, the model is applicable and adaptive on diverse conditions irrespective of battery chemistry. However, the geometric and physical properties have to be inserted with care corresponding to the new battery cell for the particular case. It helps to assess different candidate solutions for effective BTMS. It can help maintenance and diagnostic of the batteries.

## V. CONCLUSION

A unit cell based on the pack level thermal modelling framework is proposed, designed and simulated. More specifically, thermo-physical characteristics of battery cells to design a unit battery cell thermal management system is studied in detail. The research utilizes already established mathematical equations that describe the thermodynamic behavior of the cell. The carrier medium flow with forced convection is considered for simulating the cooling phenomenon. It is accomplished by laminar flow based air coolant flow inside the operating battery cell. The preliminary results of this research are presented for showing the evolutionof the hot-spots of the battery cell in a three-dimensional manner. It uses calorimetric experiment result as a base for a specified uniform heat generation inside the cell. The results demonstrate there is an increase of the temperature gradient when the applied current (load) is increased. This gradient can be reduced by a proper flow of the liquid. The result helps to understand the correlation between the heat generation and the maximal increase of surface temperature inside the battery. Based on this understanding of thermal behavior stemming from the model, temperature-control approaches for battery packs can be further developed. Using the unit cell model, pack level model models can be developed for performance simulation. Using this model and evaluating the performance of BTMS based on the calorimetric measurement may lead to the verifiable and decisive conclusion for optimal BTMS development.

## ACKNOWLEDGMENT

The authors gratefully acknowledge the financial support for this work from the Danish Strategic Research Council to the Advanced Lifetime Predictions of Battery Energy Storage (ALPBES) project.

# Appendix

TABLE II. PARAMETER LIST USED FOR THE THREE-DIMENSIONAL MODELLING OF THE BATTERY CELL(NEGATIVE VALUE MEANS EXTRUDING OUT OF SURFACE).

| Type | Name | Symbol | Value | Origin of the value |
|---|---|---|---|---|
| Geometrical Parameters | Outer Rectangle Length of cell | *len_out_rect* | 222 [mm] | Measured |
| | Outer Rectangle Width of cell | *wid_out_rect* | 214 [mm] | Measured |
| | Inner Rectangle Length of cell | *len_inn_rect* | 182 [mm] | Measured |
| | Inner Rectangle Width of cell | *wid_inn_rect* | 172 [mm] | Measured |
| | Thin layer thickness | *d_thin_lay* | 0.5e-3 [m] | Measured |
| | Thickness of the Battery | *Bat_Thickness* | 7.7 [mm] | Measured |
| | Thickness of the Electrode Conductor | *Electrode_Thickness* | 0.5 [mm] | Measured |
| | Lateral Distance of the cell | *Lateral_Distance* | 30 [mm] | Measured |
| | Axial Distance of the cell | *Axial_Distance* | 250 [mm] | Measured |
| | Width of the Holder | *Holder_width* | 20 [mm] | Measured |
| | Depth of the Holder | *Holder_depth* | 70 [mm] | Measured |
| | Height of the Holder | *Holder_height* | 25 [mm] | Measured |
| | Elevation of the holder on longitudinal Direction | *Holder_Elevation_x* | -5 [mm] | Measured |
| | Elevation of the holder on lateral Direction | *Holder_Elevation_y* | -5 [mm] | Measured |
| | Elevation of the holder on normal Direction | *Holder_Elevation_z* | -5 [mm] | Measured |
| | Fluid Width of the outer domain Box | *FluidBox_width* | 40 [mm] | Measured |
| | Fluid Depth of the outer domain Box | *FluidBox_depth* | 250 [mm] | Measured |
| | Fluid Height of the outer domain Box | *FluidBox_height* | 260 [mm] | Measured |
| | Clearance of the longitudinal edge of the outer domain fluidbox | *Clearance_x_edge_fluidbox* | -15 [mm] | Measured |
| | Clearance of the lateral edge of the outer domain fluidbox | *Clearance_y_edge_fluidbox* | -15 [mm] | Measured |
| | Clearance of the normal edge of the outer domain fluidbox | *Clearance_z_edge_fluidbox* | -15 [mm] | Measured |
| Battery electrode Physical Parameters | Positive Electrode Width | *Width_pos_electr* | 82 [mm] | Measured |
| | Positive Electrode Length | *Length_pos_electr* | 42 [mm] | Measured |
| | Negative Electrode Width | *Width_neg_electr* | 82 [mm] | Measured |
| | Positive Electrode Length | *Length_neg_electr* | 42 [mm] | Measured |
| Battery Physical Parameters | Density of Battery | *Battery_Density* | 2700 [kg/(m^3)] | Reference [38] |
| | Heat Capacity of Battery | *Battery_HeatCapacity* | 860 [J/(kg*K)] | Reference [38] |
| | Heat Source Magnitude | *q_source* | 1536 [mW] | As Measured in calorimeter |
| | Thermal Conductivity in longitudinal direction | *kxx* | 30 [$Wm^{-1}K^{-1}$] | Reference [38] |
| | Thermal Conductivity in lateral direction | *Kyy* | 30 [$Wm^{-1}K^{-1}$] | Reference [38] |
| | Thermal Conductivity in normal direction | *Kzz* | 0.16 [$Wm^{-1}K^{-1}$] | Reference [38] |
| Battery case Physical Parameters | Case Heat capacity at constant pressure | *Cp_case* | 678 [J/(kg*K)] | Multiphysics Library |
| | Case Density | *Rho_case* | 2320 [kg/(m^3)] | Multiphysics Library |
| | Case Thermal Conductivity | *K_case* | 155 [$Wm^{-1}K^{-1}$] | Multiphysics Library |
| Holder casing Physical Parameters | Holder Casing Heat capacity at constant pressure | *Cp_holdercasing* | 893 [J/(kg*K)] | Multiphysics Library |
| | Holder Casing Density | *Rho_holdercasing* | 2730 [kg/(m^3)] | Multiphysics Library |
| | Holder Casing Thermal Conductivity | *K_holdercasing* | 155 [$Wm^{-1}K^{-1}$] | Multiphysics Library |
| Positive Electrode Physical Parameters | Positive Electrode Heat capacity at constant pressure | *Cp_posElectrode* | 385 [J/(kg*K)] | Multiphysics Library |
| | Positive Electrode Density | *Rho_posElectrode* | 8700 [kg/(m^3)] | Multiphysics Library |
| | Holder Casing Thermal Conductivity | *K_posElectrode* | 400 [$Wm^{-1}K^{-1}$] | Multiphysics Library |
| Negative Electrode Physical Parameters | Negative Electrode Heat capacity at constant pressure | *Cp_negElectrode* | 900 [J/(kg*K)] | Multiphysics Library |
| | Negative Electrode Density | *Rho _ negElectrode* | 238 [kg/(m^3)] | Multiphysics Library |
| | Negative Electrode Thermal Conductivity | *K _ negElectrode* | 2700 [$Wm^{-1}K^{-1}$] | Multiphysics Library |
| Air Physical Parameters | Air Heat capacity at constant pressure | *Cp_air* | 1005 [J/(kg*K)] | Multiphysics Library |
| | Air Density | *Rho _ air* | 1.125 [kg/(m^3)] | Multiphysics Library |
| | Air Thermal Conductivity | *K _air* | 0.0271 [$Wm^{-1}K^{-1}$] | Multiphysics Library |
| Environmental Parameters | Pressure | *p* | 1 [atm] | Assumed |
| | Maximum Velocity | *umax* | 1 [m/s] | Assumed |
| | Initial Temperature | *T_init* | 27+273.16 [K] | Measured |
| | External Temperature | *T_ext* | 27+273.16 [K] | Measured |

## REFERENCES


[1] E. Prada, D. Di Domenico, Y. Creff, J. Bernard, V. Sauvant-Moynot, and F. Huet, "Simplified Electrochemical and Thermal Model of LiFePO4-Graphite Li-Ion Batteries for Fast Charge Applications," *Journal of the Electrochemical Society,* vol. 159, pp. A1508-A1519, 2012.

[2] G. Guo, B. Long, B. Cheng, S. Zhou, P. Xu, and B. Cao, "Three-dimensional thermal finite element modeling of lithium-ion battery in thermal abuse application," *Journal of Power Sources,* vol. 195, pp. 2393-2398, 2010.

[3] J. Newman, K. E. Thomas, H. Hafezi, and D. R. Wheeler, "Modeling of lithium-ion batteries," *Journal of Power Sources,* vol. 119, pp. 838-843, Jun 2003.

[4] M. R. Khan, S. J. Andreasen, and S. K. Kær. (2014, 01.08.2014) Novel Battery Thermal Management System for Greater Lifetime Ratifying Current Quality and Safety Standard. *Battery Connections*. 6-10.

[5] T. M. Bandhauer, S. Garimella, and T. F. Fuller, "A Critical Review of Thermal Issues in Lithium-Ion Batteries," *Journal of the Electrochemical Society,* vol. 158, pp. R1-R25, 2011.

[6] M. R. Khan, J. V. Barreras, A. I. Stan, M. Swierczynski, S. J. Andreasen, and S. K. Kær, "Behavior Patterns, Origin of Problems and Solutions Regarding Hysteresis Phenomena in Complex Battery Systems," in *Hysteresis: Types, Applications and Behavior Patterns in Complex Systems*, J. C. Dias, Ed., First ed: Nova Science Publishers 2014, pp. 215-226.

[7] M. R. Khan, G. Mulder, and J. Van Mierlo, "An online framework for state of charge determination of battery systems using combined system identification approach," *Journal of Power Sources,* vol. 246, pp. 629-641, 1/15/ 2014.

[8] G. Vertiz, M. Oyarbide, H. Macicior, O. Miguel, I. Cantero, P. Fernandez de Arroiabe*, et al.*, "Thermal characterization of large size lithium-ion pouch cell based on 1d electro-thermal model," *Journal of Power Sources,* vol. 272, pp. 476-484, 12/25/ 2014.

[9] J. Vetter, P. Novák, M. R. Wagner, C. Veit, K. C. Möller, J. O. Besenhard*, et al.*, "Ageing mechanisms in lithium-ion batteries," *Journal of Power Sources,* vol. 147, pp. 269-281, 9/9/ 2005.

[10] H. G. Sun, X. H. Wang, B. Tossan, and R. Dixon, "Three-dimensional thermal modeling of a lithium-ion battery pack," *Journal of Power Sources,* vol. 206, pp. 349-356, May 2012.

[11] R. Kizilel, R. Sabbah, J. R. Selman, and S. Al-Hallaj, "An alternative cooling system to enhance the safety of Li-ion battery packs," *Journal of Power Sources,* vol. 194, pp. 1105-1112, Dec 2009.

[12] C. Forgez, D. Vinh Do, G. Friedrich, M. Morcrette, and C. Delacourt, "Thermal modeling of a cylindrical LiFePO4/graphite lithium-ion battery," *Journal of Power Sources,* vol. 195, pp. 2961-2968, 2010.

[13] G. H. Kim, K. Smith, K. J. Lee, S. Santhanagopalan, and A. Pesaran, "Multi-Domain Modeling of Lithium-Ion Batteries Encompassing Multi-Physics in Varied Length Scales," *Journal of the Electrochemical Society,* vol. 158, pp. A955-A969, 2011.

[14] K. Smith, G.-H. Kim, E. Darcy, and A. Pesaran, "Thermal/electrical modeling for abuse-tolerant design of lithium ion modules," *International Journal of Energy Research,* vol. 34, pp. 204-215, 2010.

[15] K.-J. Lee, K. Smith, A. Pesaran, and G.-H. Kim, "Three dimensional thermal-, electrical-, and electrochemical-coupled model for cylindrical wound large format lithium-ion batteries," *Journal of Power Sources,* vol. 241, pp. 20-32, 2013.

[16] K. Gi-Heon, A. Pesaran, and R. Spotnitz, "A three-dimensional thermal abuse model for lithium-ion cells," *Journal of Power Sources,* vol. 170, pp. 476-489, 10 2007.

[17] J. Newman and K. E. Thomas-Alyea, *Electrochemical Systems*, 3rd Edition ed. Hoboken, New Jersey: John Wiley & Sons Inc., 2004.

[18] K. E. Thomas and J. Newman, "Heats of mixing and of entropy in porous insertion electrodes," *Journal of Power Sources,* vol. 119, pp. 844-849, Jun 2003.

[19] M. Muratori, N. Ma, M. Canova, Y. Guezennec, and Asme, *A model order reduction method for the temperature estimation in a cylindrical li-ion battery cell*. New York: Amer Soc Mechanical Engineers, 2010.

[20] A. A. Pesaran, "Battery thermal models for hybrid vehicle simulations," *Journal of Power Sources,* vol. 110, pp. 377-382, Aug 2002.

[21] A. A. Pesaran, A. Vlahinos, and S. D. Burch, "Thermal Performance of EV and HEV Battery Modules and Packs," in *14th International Electric Vehicle Symposium*, Orlando, Florida, 1997.

[22] K. Smith, G. H. Kim, E. Darcy, and A. Pesaran, "Thermal/electrical modeling for abuse-tolerant design of lithium ion modules," *International Journal of Energy Research,* vol. 34, pp. 204-215, Feb 2010.

[23] "Feasibility Study and Techno-economic Optimization Model for Battery Thermal Management System," 2014.

[24] D. H. Doughty, P. C. Butler, R. G. Jungst, and E. P. Roth, "Lithium battery thermal models," *Journal of power sources,* vol. 110, pp. 357-363, 2002.

[25] S. Al-Hallaj and J. R. Selman, "Thermal modeling of secondary lithium batteries for electric vehicle/hybrid electric vehicle applications," *Journal of Power Sources,* vol. 110, pp. 341-348, Aug 2002.

[26] S. C. Chen, C. C. Wan, and Y. Y. Wang, "Thermal analysis of lithium-ion batteries," *Journal of Power Sources,* vol. 140, pp. 111-124, Jan 2005.

[27] Y. Chen and J. W. Evans, "Heat-transfer phenomena in lithium polymer-electrolyte batteries for electric vehicle application," *Journal of the Electrochemical Society,* vol. 140, pp. 1833-1838, Jul 1993.

[28] Y. F. Chen and J. W. Evans, "3-dimensional thermal modeling of lithium-polymer batteries under galvanostatic discharge and dynamic power profile," *Journal of the Electrochemical Society,* vol. 141, pp. 2947-2955, Nov 1994.

[29] R. E. Gerver and J. P. Meyers, "Three-Dimensional Modeling of Electrochemical Performance and Heat Generation of Lithium-Ion Batteries in Tabbed Planar Configurations," *Journal of the Electrochemical Society,* vol. 158, pp. A835-A843, 2011.

[30] M. R. Khan and S. K. Kær, "Modeling Thermal Effects of Battery Cells Inside Electric Vehicle Battery Packs," in *2015 COMSOL Conference*, Grenoble, France, 2015.

[31] Z. H. Rao and S. F. Wang, "A review of power battery thermal energy management," *Renewable & Sustainable Energy Reviews,* vol. 15, pp. 4554-4571, Dec 2011.

[32] V. Ramadesigan, V. Boovaragavan, J. C. Pirkle, and V. R. Subramanian, "Efficient Reformulation of Solid-Phase Diffusion in Physics-Based Lithium-Ion Battery Models," *Journal of the Electrochemical Society,* vol. 157, pp. A854-A860, 2010.

[33] L. Rao and J. Newman, "Heat-Generation Rate and General Energy Balance for Insertion Battery Systems," *Journal of The Electrochemical Society,* vol. 144, pp. 2697-2704, 1997.

[34] T. G. Zavalis, M. Behm, and G. Lindbergh, "Investigation of Short-Circuit Scenarios in a Lithium-Ion Battery Cell," *Journal of The Electrochemical Society,* vol. 159, pp. A848-A859, 2012.

[35] K. Kumaresan, G. Sikha, and R. E. White, "Thermal model for a Li-ion cell," *Journal of The Electrochemical Society,* vol. 155, pp. A164-A171, 2008.

[36] W. Gu and C. Wang, "Thermal and electrochemical coupled modeling of a lithium-ion cell," in *GATE Center for Advanced Energy Storage, Proceedings of the ECS*, University Park, PA 16802, USA, 2000, pp. 748-762.

[37] M. R. Khan, M. J. Swierczynski, and S. K. Kær, "Determination of the Behavior and Performance of Commercial Li-Ion Pouch Cells by the means of Isothermal Calorimeter," in *Eleventh International Conference on Ecological Vehicles and Renewable Energies (EVER16)*, Grimaldi Forum, Monaco, 2016.

[38] J. Yi, U. S. Kim, C. B. Shin, T. Han, and S. Park, "Three-Dimensional Thermal Modeling of a Lithium-Ion Battery Considering the Combined Effects of the Electrical and Thermal Contact Resistances between Current Collecting Tab and Lead Wire," *Journal of the Electrochemical Society,* vol. 160, pp. A437-A443, 2013.